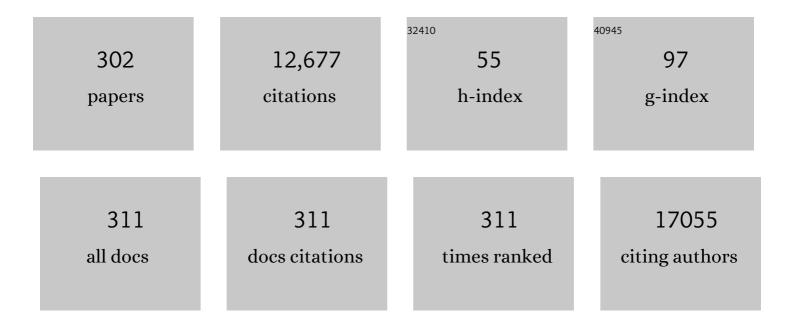
List of Publications by Year in descending order

Source: https://exaly.com/author-pdf/3178466/publications.pdf Version: 2024-02-01



#	Article	IF	CITATIONS
1	Blood clot-inspired viscoelastic fibrin gel: New aqueous binder for silicon anodes in lithium ion batteries. Energy Storage Materials, 2022, 45, 730-740.	9.5	22
2	Photovoltaic powered solar hydrogen production coupled with waste SO2 valorization enabled by MoP electrocatalysts. Applied Catalysis B: Environmental, 2022, 305, 121045.	10.8	11
3	Rational design of porous Ruâ€doped <scp>CuO</scp> nanoarray on carbon cloth: Toward reversible catalyst layer for efficient <scp> Liâ€O <sub>2</sub> </scp> batteries. International Journal of Energy Research, 2022, 46, 8120-8129.	2.2	5
4	Metal organic framework-based nanostructure materials: applications for non-lithium ion battery electrodes. CrystEngComm, 2022, 24, 2925-2947.	1.3	18
5	Elucidating the Synergistic Behavior of Orientationâ€Controlled SnS Nanoplates and Carbon Layers for Highâ€Performance Lithium―and Sodiumâ€Ion Batteries (Adv. Energy Mater. 8/2022). Advanced Energy Materials, 2022, 12, .	10.2	1
6	Elucidating the Synergistic Behavior of Orientationâ€Controlled SnS Nanoplates and Carbon Layers for Highâ€Performance Lithium―and Sodiumâ€Ion Batteries. Advanced Energy Materials, 2022, 12, .	10.2	25
7	Porous carbon cubes decorated with cobalt nanoparticles for oxygen evolution catalysis in Znâ€air batteries. International Journal of Energy Research, 2022, 46, 6755-6765.	2.2	1
8	Metal–organic-framework-derived vanadium( <scp>iii</scp> ) phosphate nanoaggregates for zinc-ion battery cathodes with long-term cycle stability. Journal of Materials Chemistry A, 2022, 10, 10638-10650.	5.2	19
9	Enhanced hydrogen evolution activities of the hollow <scp>surfaceâ€oxidized</scp> cobalt phosphide nanofiber electrocatalysts in alkaline media. International Journal of Energy Research, 2022, 46, 13035-13043.	2.2	8
10	Oneâ€pot aprotic solventâ€enabled synthesis of superionic <scp>Liâ€argyrodite</scp> solid electrolyte. International Journal of Energy Research, 2022, 46, 17644-17653.	2.2	4
11	Highly Efficient Perovskiteâ€Based Electrocatalysts for Water Oxidation in Acidic Environments: A Mini Review. Advanced Energy Materials, 2021, 11, 2002428.	10.2	92
12	Rational design of S, N Co-doped reduced graphene oxides/pyrrhotite Fe7S8 as free-standing anodes for large-scale, ultrahigh-rate and long-lifespan Li- and Na-ion batteries. Applied Surface Science, 2021, 540, 148358.	3.1	13
13	Electrospun-cellulose derived free-standing carbon nanofibers as lightweight, ultrathin, and stackable interlayers for lithium-sulfur batteries. Chemical Engineering Journal, 2021, 405, 126596.	6.6	26
14	Orthorhombically distorted perovskite SeZnO3 nanosheets as an electrocatalyst for lithium-oxygen batteries. Chemical Engineering Journal, 2021, 406, 126896.	6.6	16
15	Toxicity of orally administered foodâ€grade titanium dioxide nanoparticles. Journal of Applied Toxicology, 2021, 41, 1127-1147.	1.4	21
16	Effect of PM10 on pulmonary immune response and fetus development. Toxicology Letters, 2021, 339, 1-11.	0.4	11
17	Wide pH range electrocatalytic hydrogen evolution using molybdenum phosphide nanoparticles uniformly anchored on porous carbon cloth. Ceramics International, 2021, 47, 9347-9353.	2.3	5
18	FeSe hollow spheroids as electrocatalysts for high-rate Li–O2 battery cathodes. Journal of Alloys and Compounds, 2021, 856, 158269.	2.8	10

#	Article	IF	CITATIONS
19	Enhanced sodium storage performance of silk fibroinâ€derived hollow iron sulfide with potential window control. International Journal of Energy Research, 2021, 45, 4755-4764.	2.2	4
20	Three-dimensional construction of electrode materials using TiC nanoarray substrates for highly efficient electrogeneration of sulfate radicals and molecular hydrogen in a single electrolysis cell. Journal of Materials Chemistry A, 2021, 9, 11705-11717.	5.2	5
21	Freeâ€standing molybdenum disulfides on porous carbon cloth for lithiumâ€ion battery anodes. International Journal of Energy Research, 2021, 45, 11329-11337.	2.2	7
22	Repeated intratracheal instillation of zinc oxide nanoparticles induced pulmonary damage and a systemic inflammatory response in cynomolgus monkeys. Nanotoxicology, 2021, 15, 621-635.	1.6	4
23	Progress and Prospects on the Fabrication of Grapheneâ€Based Nanostructures for Energy Storage, Energy Conversion and Biomedical Applications. Chemistry - an Asian Journal, 2021, 16, 1365-1381.	1.7	7
24	Vertically Aligned Sulfiphilic Cobalt Disulfide Nanosheets Supported on a Free-Standing Carbon Nanofiber Interlayer for High-Performance Lithium–Sulfur Batteries. ACS Sustainable Chemistry and Engineering, 2021, 9, 8487-8496.	3.2	4
25	Fibrin biopolymer hydrogel-templated 3D interconnected Si@C framework for lithium ion battery anodes. Applied Surface Science, 2021, 551, 149439.	3.1	9
26	Ultrafine CoP nanoparticles encapsulated in N/P dual-doped carbon cubes derived from 7,7,8,8-tetracyanoquinodimethane for lithium-ion batteries. Applied Surface Science, 2021, 555, 149716.	3.1	9
27	Kinetic insight into perovskite <scp>La<sub>0.8</sub>Sr<sub>0.2</sub>VO<sub>3</sub></scp> nanofibers as an efficient electrocatalytic cathode for highâ€rate <scp>LiO<sub>2</sub></scp> batteries. InformaÄnÃ-Materiály, 2021, 3, 1295-1310.	8.5	30
28	Porous Lithiophilic Li–Si Alloyâ€Type Interfacial Framework via Selfâ€Discharge Mechanism for Stable Lithium Metal Anode with Superior Rate. Advanced Energy Materials, 2021, 11, 2101544.	10.2	56
29	TCNQ-derived N/S dual-doped carbon cube electrocatalysts with built-in CoS2 nanoparticles for high-rate lithium-oxygen batteries. Chemical Engineering Journal, 2021, 418, 129367.	6.6	6
30	Ru2P nanofibers for high-performance anion exchange membrane water electrolyzer. Chemical Engineering Journal, 2021, 420, 130491.	6.6	19
31	Multiple pathways of alveolar macrophage death contribute to pulmonary inflammation induced by silica nanoparticles. Nanotoxicology, 2021, 15, 1087-1101.	1.6	12
32	Amorphous hydrated vanadium oxide with enlarged interlayer spacing for aqueous zinc-ion batteries. Chemical Engineering Journal, 2021, 420, 130528.	6.6	42
33	Vertically aligned Si@reduced graphene oxide frameworks for <scp>binderâ€free highâ€arealâ€capacity Liâ€ion</scp> battery anodes. International Journal of Energy Research, 2021, 45, 9704-9712.	2.2	4
34	Mechanically Interlocked Polymer Electrolyte with Builtâ€In Fast Molecular Shuttles for Allâ€Solidâ€State Lithium Batteries. Advanced Energy Materials, 2021, 11, 2102583.	10.2	27
35	Porous Lithiophilic Li–Si Alloyâ€Type Interfacial Framework via Selfâ€Discharge Mechanism for Stable Lithium Metal Anode with Superior Rate (Adv. Energy Mater. 37/2021). Advanced Energy Materials, 2021, 11, 2170146.	10.2	2
36	Mechanically Interlocked Polymer Electrolyte with Builtâ€In Fast Molecular Shuttles for Allâ€Solidâ€State Lithium Batteries (Adv. Energy Mater. 44/2021). Advanced Energy Materials, 2021, 11, 2170173.	10.2	0

#	Article	IF	CITATIONS
37	Back Cover Image. InformaÄnÃ-Materiály, 2021, 3, .	8.5	0
38	Nickel disulfide nanosheet as promising cathode electrocatalyst for long-life lithium–oxygen batteries. Energy Storage Materials, 2020, 24, 594-601.	9.5	21
39	Silica-templated hierarchically porous carbon modified separators for lithium–sulfur batteries with superior cycling stabilities. Journal of Power Sources, 2020, 448, 227462.	4.0	25
40	Electrocatalytic Selective Oxygen Evolution of Carbon-Coated Na <sub>2</sub> Co <sub>1–<i>x</i></sub> Fe <sub><i>x</i></sub> P <sub>2</sub> O <sub>7</sub> Nanoparticles for Alkaline Seawater Electrolysis. ACS Catalysis, 2020, 10, 702-709.	5.5	141
41	Inhaled underground subway dusts may stimulate multiple pathways of cell death signals and disrupt immune balance. Environmental Research, 2020, 191, 109839.	3.7	6
42	A synergistic engineering layer with a versatile H <sub>2</sub> Ti <sub>3</sub> O <sub>7</sub> electrocatalyst for a suppressed shuttle effect and enhanced catalytic conversion in lithium–sulfur batteries. Journal of Materials Chemistry A, 2020, 8, 25411-25424.	5.2	18
43	Organogermanium Nanowire Cathodes for Efficient Lithium–Oxygen Batteries. ACS Nano, 2020, 14, 15894-15903.	7.3	8
44	Peroxymonosulfate activation by carbon-encapsulated metal nanoparticles: Switching the primary reaction route and increasing chemical stability. Applied Catalysis B: Environmental, 2020, 279, 119360.	10.8	60
45	Formation of lamellar body-like structure may be an initiator of didecyldimethylammonium chloride-induced toxic response. Toxicology and Applied Pharmacology, 2020, 404, 115182.	1.3	6
46	In Situ Conversion of Metal–Organic Frameworks into VO <sub>2</sub> –V <sub>3</sub> S <sub>4</sub> Heterocatalyst Embedded Layered Porous Carbon as an "Allâ€inâ€One―Host for Lithium–Sulfur Batteries. Small, 2020, 16, e2004806.	5.2	35
47	High-power lithium-ion capacitor using orthorhombic Nb2O5 nanotubes enabled by cellulose-based electrospun scaffolds. Cellulose, 2020, 27, 9991-10006.	2.4	3
48	Highly active and stable electrocatalytic transition metal phosphides ( <scp> Ni <sub>2</sub> P </scp> ) Tj ETQq0 current density. International Journal of Energy Research, 2020, 44, 11894-11907.	0 0 rgBT / 2.2	Overlock 10 7
49	Separators Modified Using MoO <sub>2</sub> @Carbon Nanotube Nanocomposites as Dual-Mode Li-Polysulfide Anchoring Materials for High-Performance Anti-Self-Discharge Lithium–Sulfur Batteries. ACS Sustainable Chemistry and Engineering, 2020, 8, 15134-15148.	3.2	18
50	Sodiumâ€nickel pyrophosphate as a novel oxygen evolution electrocatalyst in alkaline medium. Journal of the American Ceramic Society, 2020, 103, 4748-4753.	1.9	6
51	Waste glass microfiber filter-derived fabrication of fibrous yolk-shell structured silicon/carbon composite freestanding electrodes for lithium-ion battery anodes. Journal of Power Sources, 2020, 468, 228407.	4.0	28
52	Metal-organic-framework-derived 3D crumpled carbon nanosheets with self-assembled CoxSy nanocatalysts as an interlayer for lithium-sulfur batteries. Chemical Engineering Journal, 2020, 400, 125959.	6.6	35
53	Carbon-coated tungsten diselenide nanosheets uniformly assembled on porous carbon cloth as flexible binder-free anodes for sodium-ion batteries with improved electrochemical performance. Journal of Alloys and Compounds, 2020, 827, 154348.	2.8	16
54	Cobalt phosphide nanoarrays with crystalline-amorphous hybrid phase for hydrogen production in universal-pH. Nano Research, 2020, 13, 2469-2477.	5.8	54

#	Article	IF	CITATIONS
55	Redox effect of Fe2+/Fe3+ in iron phosphates for enhanced electrocatalytic activity in Li-O2 batteries. Chemical Engineering Journal, 2020, 388, 124294.	6.6	22
56	Dynamic evolution of a hydroxylated layer in ruthenium phosphide electrocatalysts for an alkaline hydrogen evolution reaction. Journal of Materials Chemistry A, 2020, 8, 5655-5662.	5.2	25
57	Efficient waste polyvinyl(butyral) and cellulose composite enabled carbon nanofibers for oxygen reduction reaction and water remediation. Applied Surface Science, 2020, 510, 145505.	3.1	13
58	Repeated-oral dose toxicity of polyethylene microplastics and the possible implications on reproduction and development of the next generation. Toxicology Letters, 2020, 324, 75-85.	0.4	120
59	Amorphous silica nanoparticle-induced pulmonary inflammatory response depends on particle size and is sex-specific in rats. Toxicology and Applied Pharmacology, 2020, 390, 114890.	1.3	10
60	A Finite Element Simulation for Induction Heat Treatment of Automotive Drive Shaft. ISIJ International, 2020, 60, 1333-1341.	0.6	4
61	Waste Liquid-Crystal Display Glass-Directed Fabrication of Silicon Particles for Lithium-Ion Battery Anodes. ACS Sustainable Chemistry and Engineering, 2019, 7, 15329-15338.	3.2	13
62	"Brainâ€Coralâ€Like―Mesoporous Hollow CoS <sub>2</sub> @Nâ€Doped Graphitic Carbon Nanoshells as Efficient Sulfur Reservoirs for Lithium–Sulfur Batteries. Advanced Functional Materials, 2019, 29, 1903712.	7.8	108
63	Lithiumâ€Sulfur Batteries: "Brainâ€Coralâ€Like―Mesoporous Hollow CoS <sub>2</sub> @Nâ€Doped Graphi Carbon Nanoshells as Efficient Sulfur Reservoirs for Lithium–Sulfur Batteries (Adv. Funct. Mater.) Tj ETQq1 1 0.	tic 7848814 I	rgBT  Overloc
64	Onion-like crystalline WS2 nanoparticles anchored on graphene sheets as high-performance anode materials for lithium-ion batteries. Chemical Engineering Journal, 2019, 375, 122033.	6.6	49
65	Synthesis and characterization of uniform hollow TiO2 nanofibers using electrospun fibrous cellulosic templates for lithium-ion battery electrodes. Journal of Alloys and Compounds, 2019, 800, 483-489.	2.8	26
66	CeO2/Co(OH)2 hybrid electrocatalysts for efficient hydrogen and oxygen evolution reaction. Journal of Alloys and Compounds, 2019, 800, 450-455.	2.8	53
67	Comparative study on ternary spinel cathode Zn–Mn–O microspheres for aqueous rechargeable zinc-ion batteries. Journal of Alloys and Compounds, 2019, 800, 478-482.	2.8	23
68	Superior anodic oxidation in tailored Sb-doped SnO2/RuO2 composite nanofibers for electrochemical water treatment. Journal of Catalysis, 2019, 374, 118-126.	3.1	31
69	Hierarchical Zn <sub>1.67</sub> Mn <sub>1.33</sub> O <sub>4</sub> /graphene nanoaggregates as new anode material for lithium-ion batteries. International Journal of Energy Research, 2019, 43, 1735-1746.	2.2	11
70	Ultrafine αâ€Phase Molybdenum Carbide Decorated with Platinum Nanoparticles for Efficient Hydrogen Production in Acidic and Alkaline Media. Advanced Science, 2019, 6, 1802135.	5.6	54
71	S,N co-doped reduced graphene oxide sheets with cobalt hydroxide nanocrystals for highly active and stable bifunctional oxygen catalysts. Inorganic Chemistry Frontiers, 2019, 6, 3501-3509.	3.0	8
72	Cellulose-derived tin-oxide-nanoparticle-embedded carbon fibers as binder-free flexible Li-ion battery anodes. Cellulose, 2019, 26, 2557-2571.	2.4	23

#	Article	IF	CITATIONS
73	Lithium–Oxygen Batteries: Tailored Porous ZnCo <sub>2</sub> O <sub>4</sub> Nanofibrous Electrocatalysts for Lithium–Oxygen Batteries (Adv. Mater. Interfaces 4/2018). Advanced Materials Interfaces, 2018, 5, 1870015.	1.9	2
74	Thermally reduced <scp>rGO</scp> â€wrapped CoP/Co <sub>2</sub> P hybrid microflower as an electrocatalyst for hydrogen evolution reaction. Journal of the American Ceramic Society, 2018, 101, 3749-3754.	1.9	24
75	Magnéli-Phase Ti <sub>4</sub> O <sub>7</sub> Nanosphere Electrocatalyst Support for Carbon-Free Oxygen Electrodes in Lithium–Oxygen Batteries. ACS Catalysis, 2018, 8, 2601-2610.	5.5	50
76	Waste Windshield-Derived Silicon/Carbon Nanocomposites as High-Performance Lithium-Ion Battery Anodes. Scientific Reports, 2018, 8, 960.	1.6	38
77	Controlled phase stability of highly Na-active triclinic structure in nanoscale high-voltage Na 2-2x Co 1+x P 2 O 7 cathode for Na-ion batteries. Journal of Power Sources, 2018, 377, 121-127.	4.0	8
78	Fast adsorption kinetics of highly dispersed ultrafine nickel/carbon nanoparticles for organic dye removal. Applied Surface Science, 2018, 439, 364-370.	3.1	67
79	Tailored Porous ZnCo <sub>2</sub> O <sub>4</sub> Nanofibrous Electrocatalysts for Lithium–Oxygen Batteries. Advanced Materials Interfaces, 2018, 5, 1701234.	1.9	9
80	Carbon-encapsulated multi-phase nanocomposite of W <sub>2</sub> C@WC <sub>1â^'x</sub> as a highly active and stable electrocatalyst for hydrogen generation. Nanoscale, 2018, 10, 21123-21131.	2.8	26
81	Single and polycrystalline CeO <sub>2</sub> nanorods as oxygen-electrode materials for lithium–oxygen batteries. Nanoscale, 2018, 10, 21292-21297.	2.8	14
82	3D Architectures of Quaternary Coâ€Niâ€Sâ€P/Graphene Hybrids as Highly Active and Stable Bifunctional Electrocatalysts for Overall Water Splitting. Advanced Energy Materials, 2018, 8, 1802319.	10.2	107
83	Synergistic Effect of CuGeO <sub>3</sub> /Graphene Composites for Efficient Oxygen–Electrode Electrocatalysts in Li–O <sub>2</sub> Batteries. Advanced Energy Materials, 2018, 8, 1801930.	10.2	37
84	Carbon-encapsulated NiFe nanoparticles as a bifunctional electrocatalyst for high-efficiency overall water splitting. Journal of Catalysis, 2018, 366, 266-274.	3.1	54
85	3D Architectures of Co <i><sub>x</sub></i> P Using Silk Fibroin Scaffolds: An Active and Stable Electrocatalyst for Hydrogen Generation in Acidic and Alkaline Media. Small, 2018, 14, e1801284.	5.2	32
86	Revisiting the conversion reaction in ultrafine SnO2 nanoparticles for exceptionally high-capacity Li-ion battery anodes: The synergetic effect of graphene and copper. Journal of Alloys and Compounds, 2018, 769, 1113-1120.	2.8	9
87	Fabrication of Mo/MoO2@carbon cloth as a flexible anode for Li-ion batteries using water-stable nanoink. Carbon, 2018, 139, 1160-1164.	5.4	8
88	Oxygen-vacancy-modified brookite TiO2 nanorods as visible-light-responsive photocatalysts. Materials Letters, 2018, 232, 146-149.	1.3	17
89	Comparison of subchronic immunotoxicity of four different types of aluminumâ€based nanoparticles. Journal of Applied Toxicology, 2018, 38, 575-584.	1.4	12
90	Enhanced cycle stability of silicon coated with waste poly(vinyl butyral)-directed carbon for lithium-ion battery anodes. Journal of Alloys and Compounds, 2017, 698, 525-531.	2.8	22

#	Article	IF	CITATIONS
91	Superior lithium storage in nitrogen-doped carbon nanofibers with open-channels. Chemical Engineering Journal, 2017, 315, 1-9.	6.6	28
92	Pulmonary glass particles may persist in the lung suppressing function of immune cells. Environmental Toxicology, 2017, 32, 1688-1700.	2.1	2
93	An approach to flexible Na-ion batteries with exceptional rate capability and long lifespan using Na <sub>2</sub> FeP <sub>2</sub> O <sub>7</sub> nanoparticles on porous carbon cloth. Journal of Materials Chemistry A, 2017, 5, 5502-5510.	5.2	64
94	MnMoO <sub>4</sub> Electrocatalysts for Superior Longâ€Life and Highâ€Rate Lithiumâ€Oxygen Batteries. Advanced Energy Materials, 2017, 7, 1601741.	10.2	53
95	Synthesis of Cu <sub>3</sub> (MoO <sub>4</sub> ) <sub>2</sub> (OH) <sub>2</sub> nanostructures by simple aqueous precipitation: understanding the fundamental chemistry and growth mechanism. CrystEngComm, 2017, 19, 154-165.	1.3	17
96	Tissue distribution following 28 day repeated oral administration of aluminumâ€based nanoparticles with different properties and the in vitro toxicity. Journal of Applied Toxicology, 2017, 37, 1408-1419.	1.4	9
97	Uniform Si nanoparticle-embedded nitrogen-doped carbon nanofiber electrodes for lithium ion batteries. Journal of Alloys and Compounds, 2017, 728, 490-496.	2.8	27
98	Fe-based hybrid electrocatalysts for nonaqueous lithium-oxygen batteries. Scientific Reports, 2017, 7, 9495.	1.6	11
99	Mo-MoO3-graphene nanocomposites as anode materials for lithium-ion batteries: scalable, facile preparation and characterization. Electrochimica Acta, 2017, 251, 81-90.	2.6	35
100	Superior sodium storage performance of reduced graphene oxide-supported Na <sub>3.12</sub> Fe <sub>2.44</sub> (P <sub>2</sub> O <sub>7</sub> ) <sub>2</sub> /C nanocomposites. Chemical Communications, 2017, 53, 9316-9319.	2.2	25
101	Carbon-decorated iron oxide hollow granules formed using a silk fibrous template: lithium-oxygen battery and wastewater treatment applications. NPG Asia Materials, 2017, 9, e450-e450.	3.8	21
102	Synthesis of Flowerâ€like Cu <sub>3</sub> [MoO <sub>4</sub> ] <sub>2</sub> O from Cu <sub>3</sub> (MoO <sub>4</sub> ) <sub>2</sub> (OH) <sub>2</sub> and Its Application for Lithiumâ€lon Batteries: Structureâ€Electrochemical Property Relationships. ChemElectroChem, 2017, 4, 2608-2617.	1.7	9
103	Tailored silicon hollow spheres with Micrococcus for Li ion battery electrodes. Chemical Engineering Journal, 2017, 327, 297-306.	6.6	34
104	Fabrication of highly porous carbon as sulfur hosts using waste green tea bag powder for lithium–sulfur batteries. Ceramics International, 2017, 43, 2836-2841.	2.3	17
105	Pulmonary persistence of graphene nanoplatelets may disturb physiological and immunological homeostasis. Journal of Applied Toxicology, 2017, 37, 296-309.	1.4	28
106	Electrocatalytic performance of CuO/graphene nanocomposites for Li–O 2 batteries. Journal of Alloys and Compounds, 2017, 707, 275-280.	2.8	14
107	Biodistribution and toxicity of spherical aluminum oxide nanoparticles. Journal of Applied Toxicology, 2016, 36, 424-433.	1.4	42
108	Three-Dimensional Hybrid Tin Oxide/Carbon Nanowire Arrays for High-Performance Li Ion Battery Electrodes. Journal of Nanoscience and Nanotechnology, 2016, 16, 10588-10591.	0.9	2

#	Article	IF	CITATIONS
109	Enhanced Lithium Storage in Hierarchically Porous Carbon Derived from Waste Tea Leaves. Scientific Reports, 2016, 6, 39099.	1.6	37
110	A higher aspect ratio enhanced bioaccumulation and altered immune responses due to intravenously-injected aluminum oxide nanoparticles. Journal of Immunotoxicology, 2016, 13, 439-448.	0.9	13
111	One-pot low-temperature sonochemical synthesis of CuO nanostructures and their electrochemical properties. Ceramics International, 2016, 42, 19454-19460.	2.3	15
112	Li-electroactivity of thermally-reduced V2O3 nanoparticles. Materials Letters, 2016, 180, 243-246.	1.3	15
113	Enhanced Lithium Storage in Reduced Graphene Oxide-supported M-phase Vanadium(IV) Dioxide Nanoparticles. Scientific Reports, 2016, 6, 30202.	1.6	22
114	Heteroepitaxy-Induced Rutile VO <sub>2</sub> with Abundantly Exposed (002) Facets for High Lithium Electroactivity. ACS Energy Letters, 2016, 1, 216-224.	8.8	23
115	Comparison of distribution and toxicity following repeated oral dosing of different vanadium oxide nanoparticles in mice. Environmental Research, 2016, 150, 154-165.	3.7	24
116	Glass-frit size dependence of densification behavior and mechanical properties of zinc aluminum calcium borosilicate glass-ceramics. Journal of Alloys and Compounds, 2016, 686, 95-100.	2.8	5
117	Fabrication of sulfur-impregnated porous carbon nanostructured electrodes via dual-mode activation for lithium–sulfur batteries. Materials Letters, 2016, 172, 116-119.	1.3	15
118	Synthesis of Silicon Carbide Nanocrystals Using Waste Poly(vinyl butyral) Sheet. Journal of the American Ceramic Society, 2016, 99, 1885-1888.	1.9	14
119	Enhanced Li- and Na-storage in Sb-Graphene nanocomposite anodes. Materials Research Bulletin, 2016, 76, 338-343.	2.7	26
120	Stable high-areal-capacity nanoarchitectured germanium anodes on three-dimensional current collectors for Li ion microbatteries. Journal of Materials Chemistry A, 2016, 4, 1060-1067.	5.2	17
121	High-power and long-life supercapacitive performance of hierarchical, 3-D urchin-like W18O49 nanostructure electrodes. Nano Research, 2016, 9, 633-643.	5.8	47
122	Windshield-waste-driven synthesis of hydroxy sodalite. Journal of the Ceramic Society of Japan, 2015, 123, 1022-1026.	0.5	3
123	Synthesis of uniform-sized zeolite from windshield waste. Materials Chemistry and Physics, 2015, 166, 20-25.	2.0	13
124	Highly stable sodium storage in 3-D gradational Sb–NiSb–Ni heterostructures. Nano Energy, 2015, 15, 479-489.	8.2	37
125	Synthesis of carbon-incorporated titanium oxide nanocrystals by pulsed solution plasma: electrical, optical investigation and nanocrystals analysis. RSC Advances, 2015, 5, 9497-9502.	1.7	4
126	Comparison of the toxicity of aluminum oxide nanorods with different aspect ratio. Archives of Toxicology, 2015, 89, 1771-1782.	1.9	24

#	Article	IF	CITATIONS
127	Biomineralized Multifunctional Magnetite/Carbon Microspheres for Applications in Li″on Batteries and Water Treatment. Chemistry - A European Journal, 2015, 21, 4655-4663.	1.7	12
128	High-areal-capacity lithium storage of the Kirkendall effect-driven hollow hierarchical NiSxnanoarchitecture. Nanoscale, 2015, 7, 2790-2796.	2.8	38
129	Structural and electrochemical characteristics of morphology-controlled Li[Ni0.5Mn1.5]O4 cathodes. Electrochimica Acta, 2015, 156, 29-37.	2.6	34
130	Toxic response of graphene nanoplatelets in vivo and in vitro. Archives of Toxicology, 2015, 89, 1557-1568.	1.9	86
131	Examination of graphene nanoplatelets as cathode materials for lithium–oxygen batteries by differential electrochemical mass spectrometry. Electrochemistry Communications, 2015, 57, 39-42.	2.3	16
132	Superior long-life and high-rate Ge nanoarrays anchored on Cu/C nanowire frameworks for Li-ion battery electrodes. Nano Energy, 2015, 13, 218-225.	8.2	33
133	Reversible Li-storage in Titanium(III) Oxide Nanosheets. Electrochimica Acta, 2015, 170, 25-32.	2.6	14
134	Three-Dimensional Numerical Model Considering Phase Transformation in Friction Stir Welding of Steel. Metallurgical and Materials Transactions A: Physical Metallurgy and Materials Science, 2015, 46, 6040-6051.	1.1	9
135	Facile synthesis and electroactivity of 3-D hierarchically superstructured cobalt orthophosphate for lithium-ion batteries. Journal of Alloys and Compounds, 2015, 652, 100-105.	2.8	13
136	Comparison of catalytic performance of different types of graphene in Li–O2 batteries. Journal of Alloys and Compounds, 2015, 647, 231-237.	2.8	22
137	Li2MnSiO4 nanorods-embedded carbon nanofibers for lithium-ion battery electrodes. Electrochimica Acta, 2015, 180, 756-762.	2.6	22
138	Morphology-controlled solvothermal synthesis of Li2FeSiO4 nanoparticles for Li-ion battery cathodes. Materials Letters, 2015, 160, 507-510.	1.3	6
139	Ta-substituted SnNb <sub>2â^'x</sub> Ta <sub>x</sub> O <sub>6</sub> photocatalysts for hydrogen evolution under visible light irradiation. Journal of Materials Chemistry A, 2015, 3, 825-831.	5.2	18
140	Transformation plasticity in boron-bearing low carbon steel. Metals and Materials International, 2015, 21, 799-804.	1.8	4
141	Preparation of cobalt nanoparticles from polymorphic bacterial templates: A novel platform for biocatalysis. International Journal of Biological Macromolecules, 2015, 81, 747-753.	3.6	12
142	Superior high rate capability of size-controlled LiMnPO4/C nanosheets with preferential orientation. RSC Advances, 2015, 5, 100709-100714.	1.7	11
143	Tailoring uniform Î <sup>3</sup> -MnO2 nanosheets on highly conductive three-dimensional current collectors for high-performance supercapacitor electrodes. Nano Research, 2015, 8, 990-1004.	5.8	39
144	Finite Element Investigation for Edge Wave Prediction in Hot Rolled Steel during Run Out Table Cooling. ISIJ International, 2014, 54, 1646-1652.	0.6	22

#	Article	IF	CITATIONS
145	Preparation and Characterizations of Lithium Iron Borate Nano-sized Powders via Aerosol and Thermal Process. Current Nanoscience, 2014, 10, 168-170.	0.7	4
146	Electrospun Cu/Sn/C Nanocomposite Fiber Anodes with Superior Usable Lifetime for Lithium―and Sodiumâ€Ion Batteries. Chemistry - an Asian Journal, 2014, 9, 3313-3318.	1.7	18
147	Synthesis of multiphase SnSb nanoparticles-on-SnO2/Sn/C nanofibers for use in Li and Na ion battery electrodes. Electrochemistry Communications, 2014, 46, 124-127.	2.3	56
148	Timeâ€dependent bioaccumulation of distinct rodâ€type TiO <sub>2</sub> nanoparticles: Comparison by crystalline phase. Journal of Applied Toxicology, 2014, 34, 1265-1270.	1.4	9
149	Enhanced Cycle Stability of Magnetite/Carbon Nanoparticles for Li Ion Battery Electrodes. Journal of the American Ceramic Society, 2014, 97, 1413-1420.	1.9	10
150	One-pot synthesis of Fe3O4/Fe/MWCNT nanocomposites via electrical wire pulse for Li ion battery electrodes. Journal of Alloys and Compounds, 2014, 606, 204-207.	2.8	19
151	Adsorption of microbial esterases on Bacillus subtilis-templated cobalt oxide nanoparticles. International Journal of Biological Macromolecules, 2014, 65, 188-192.	3.6	12
152	Sn self-doped α-Fe2O3 nanobranch arrays supported on a transparent, conductive SnO2 trunk to improve photoelectrochemical water oxidation. International Journal of Hydrogen Energy, 2014, 39, 16459-16467.	3.8	34
153	Growth of anatase and rutile TiO2@Sb:SnO2 heterostructures and their application in photoelectrochemical water splitting. International Journal of Hydrogen Energy, 2014, 39, 17508-17516.	3.8	13
154	Surface-area-tuned, quantum-dot-sensitized heterostructured nanoarchitectures for highly efficient photoelectrodes. Nano Research, 2014, 7, 144-153.	5.8	25
155	Enhanced electrochemical performance of carbon-coated Li2MnSiO4 nanoparticles synthesized by tartaric acid-assisted sol–gel process. Ceramics International, 2014, 40, 9413-9418.	2.3	4
156	Hierarchical assembly of TiO2–SrTiO3 heterostructures on conductive SnO2 backbone nanobelts for enhanced photoelectrochemical and photocatalytic performance. Journal of Hazardous Materials, 2014, 275, 10-18.	6.5	37
157	Enhanced electroactivity with Li in Fe3O4/MWCNT nanocomposite electrodes. Journal of Alloys and Compounds, 2014, 615, S397-S400.	2.8	3
158	Highly Reversible Li Storage in Hybrid NiO/Ni/Graphene Nanocomposites Prepared by an Electrical Wire Explosion Process. ACS Applied Materials & Interfaces, 2014, 6, 137-142.	4.0	69
159	Comparison of toxicity of different nanorodâ€ŧype TiO <sub>2</sub> polymorphs <i>in vivo</i> and <i>in vitro</i> . Journal of Applied Toxicology, 2014, 34, 357-366.	1.4	21
160	Sheet-type titania, but not P25, induced paraptosis accompanying apoptosis in murine alveolar macrophage cells. Toxicology Letters, 2014, 230, 69-79.	0.4	13
161	Oleic-acid-assisted carbon coating on Sn nanoparticles for Li ion battery electrodes with long-term cycling stability. RSC Advances, 2014, 4, 44563-44567.	1.7	17
162	Facile synthesis of heterogeneous Ni-Si@C nanocomposites as high-performance anodes for Li-ion batteries. Electrochimica Acta, 2014, 146, 60-67.	2.6	15

#	Article	IF	CITATIONS
163	Anion-controlled synthesis of TiO2 nano-aggregates for Li ion battery electrodes. Materials Characterization, 2014, 96, 13-20.	1.9	9
164	Synthesis of Multiphase Cu <sub>3</sub> Ge/GeO <sub><i>x</i></sub> /CuGeO <sub>3</sub> Nanowires for Use as Lithiumâ€ion Battery Anodes. ChemElectroChem, 2014, 1, 673-678.	1.7	20
165	Three-Dimensional Hierarchical Li <sub>4</sub> Ti <sub>5</sub> O <sub>12</sub> Nanoarchitecture by a Simple Hydrothermal Method. Journal of Nanoscience and Nanotechnology, 2014, 14, 9307-9312.	0.9	1
166	Germanium microflower-on-nanostem as a high-performance lithium ion battery electrode. Scientific Reports, 2014, 4, 6883.	1.6	16
167	Synthesis and characterization of LiMnBO3 cathode material for lithium ion batteries. Current Applied Physics, 2013, 13, 1440-1443.	1.1	24
168	Hydrothermal Realization of a Hierarchical, Flowerlike MnWO <sub>4</sub> @MWCNTs Nanocomposite with Enhanced Reversible Li Storage as a New Anode Material. Chemistry - an Asian Journal, 2013, 8, 2851-2858.	1.7	17
169	Self-supported multi-walled carbon nanotube-embedded silicon nanoparticle films for anodes of Li-ion batteries. Materials Research Bulletin, 2013, 48, 1732-1736.	2.7	21
170	A novel green-emitting Ca15(PO4)2(SiO4)6:Eu2+ phosphor for applications in n-UV based w-LEDs. Materials Chemistry and Physics, 2013, 139, 350-354.	2.0	13
171	Preparation and characterization of nano-sized Y3Al5O12:Ce3+ phosphor by high-energy milling process. Current Applied Physics, 2013, 13, S69-S74.	1.1	16
172	Scalable One-pot Bacteria-templating Synthesis Route toward Hierarchical, Porous-Co3O4 Superstructures for Supercapacitor Electrodes. Scientific Reports, 2013, 3, 2325.	1.6	109
173	Fabrication and electrochemical performance of Sn-Based nanocomposite fibers via electrospinning. Electronic Materials Letters, 2013, 9, 775-777.	1.0	4
174	Tailoring nanobranches in three-dimensional hierarchical rutile heterostructures: a case study of TiO2–SnO2. CrystEngComm, 2013, 15, 2939.	1.3	19
175	Luminescent Properties of RbSrPO <sub>4</sub> :Eu <sup>2+</sup> Phosphors for Nearâ€UVâ€Based Whiteâ€Lightâ€Emitting Diodes. European Journal of Inorganic Chemistry, 2013, 2013, 4662-4666.	1.0	9
176	Controlled synthesis and Li-electroactivity of rutile TiO2 nanostructure with walnut-like morphology. Dalton Transactions, 2013, 42, 4278.	1.6	8
177	Room-temperature synthesis of CuO/graphene nanocomposite electrodes for high lithium storage capacity. Ceramics International, 2013, 39, 1749-1755.	2.3	41
178	Synthesis and Li electroactivity of dandelion-like nanorutile. Ceramics International, 2013, 39, 3459-3462.	2.3	2
179	Enhancement of fluorescence by Ce3+ doping in green-emitting Ca15(PO4)2(SiO4)6:Eu2+ phosphor for UV-based w-LEDs. Ceramics International, 2013, 39, 9791-9795.	2.3	8
180	Comparison of toxicity between the different-type TiO2 nanowires in vivo and in vitro. Archives of Toxicology, 2013, 87, 1219-1230.	1.9	33

#	Article	IF	CITATIONS
181	Nanocomposite Li-ion battery anodes consisting of multiwalled carbon nanotubes that anchor CoO nanoparticles. Materials Letters, 2013, 104, 13-16.	1.3	20
182	Heteroepitaxial growth of ZnO nanosheet bands on ZnCo2O4 submicron rods toward high-performance Li ion battery electrodes. Nano Research, 2013, 6, 348-355.	5.8	60
183	γ-Al2O3 nanospheres-directed synthesis of monodispersed BaAl2O4:Eu2+ nanosphere phosphors. CrystEngComm, 2013, 15, 4797.	1.3	11
184	RbBaPO <sub>4</sub> :Eu <sup>2+</sup> : a new alternative blue-emitting phosphor for UV-based white light-emitting diodes. Journal of Materials Chemistry C, 2013, 1, 500-505.	2.7	96
185	Synthesis and Li Electroactivity of MnS/Carbon Nanotube Composites. Journal of the Korean Ceramic Society, 2013, 50, 539-544.	1.1	2
186	Hydrothermal synthesis and electrochemical properties of FeNbO <sub>4</sub> nanospheres. Journal of the Ceramic Society of Japan, 2012, 120, 82-85.	0.5	12
187	Synthesis and Li electroactivity of Fe2P2O7 microspheres composed of self-assembled nanorods. Ceramics International, 2012, 38, 6927-6930.	2.3	12
188	Three-dimensional hierarchical self-supported multi-walled carbon nanotubes/tin(iv) disulfide nanosheets heterostructure electrodes for high power Li ion batteries. Journal of Materials Chemistry, 2012, 22, 9330.	6.7	44
189	Direct assembly of tin–MWCNT 3D-networked anode for rechargeable lithium ion batteries. RSC Advances, 2012, 2, 3315.	1.7	44
190	Template-free synthesis of monodispersed Y3Al5O12:Ce3+ nanosphere phosphor. Journal of Materials Chemistry, 2012, 22, 12275.	6.7	17
191	Biomineralized Sn-based multiphasic nanostructures for Li-ion battery electrodes. Nanoscale, 2012, 4, 4694.	2.8	37
192	A binder-free Ge-nanoparticle anode assembled on multiwalled carbon nanotube networks for Li-ion batteries. Chemical Communications, 2012, 48, 7061.	2.2	90
193	Synthesis of graphene nanosheets by the electrolytic exfoliation of graphite andÂtheir direct assembly for lithium ion battery anodes. Materials Chemistry and Physics, 2012, 135, 309-316.	2.0	15
194	Luminescent properties of phosphor converted LED using an orange-emitting Rb2CaP2O7:Eu2+ phosphor. Materials Research Bulletin, 2012, 47, 4522-4526.	2.7	20
195	Sb:SnO <sub>2</sub> @TiO <sub>2</sub> Heteroepitaxial Branched Nanoarchitectures for Li Ion Battery Electrodes. Journal of Physical Chemistry C, 2012, 116, 21717-21726.	1.5	45
196	Superior long-term cycling stability of SnO <sub>2</sub> nanoparticle/multiwalled carbon nanotube heterostructured electrodes for Li-ion rechargeable batteries. Nanotechnology, 2012, 23, 465402.	1.3	22
197	Synthesis of core/shell spinel ferrite/carbon nanoparticles with enhanced cycling stability for lithium ion battery anodes. Nanotechnology, 2012, 23, 125402.	1.3	61
198	Synthesis of pseudobrookite-type Fe2TiO5 nanoparticles and their Li-ion electroactivity. Ceramics International, 2012, 38, 6009-6013.	2.3	51

#	Article	IF	CITATIONS
199	Electrochemical performance of Ni x Co1-xMoO4 (0 ≤ ≤) nanowire anodes for lithium-ion batteries. Nanoscale Research Letters, 2012, 7, 35.	3.1	46
200	Fabrication of core/shell ZnWO4/carbon nanorods and their Li electroactivity. Nanoscale Research Letters, 2012, 7, 9.	3.1	15
201	Enhancement of cyclability of urchin-like rutile TiO2 submicron spheres by nanopainting with carbon. Journal of Materials Chemistry, 2012, 22, 15981.	6.7	60
202	Enhanced photoluminescence property of Dy3+ co-doped BaAl2O4:Eu2+ green phosphors. Ceramics International, 2012, 38, 443-447.	2.3	40
203	1D/2D carbon nanotube/graphene nanosheet composite anodes fabricated using electrophoretic assembly. Ceramics International, 2012, 38, 3017-3021.	2.3	43
204	Luminescence properties of Ca5(PO4)2SiO4:Eu2+ green phosphor for near UV-based white LED. Materials Letters, 2012, 70, 37-39.	1.3	58
205	Facile synthesis of nano-Li4 Ti5O12 for high-rate Li-ion battery anodes. Nanoscale Research Letters, 2012, 7, 10.	3.1	20
206	Size-controlled synthesis of monodispersed mesoporous α-Alumina spheres by a template-free forced hydrolysis method. Dalton Transactions, 2011, 40, 6901.	1.6	35
207	Sn-induced low-temperature growth of Ge nanowire electrodes with a large lithium storage capacity. Nanoscale, 2011, 3, 3371.	2.8	67
208	Synthesis of manganese oxide nanostructures using bacterial soft templates. CrystEngComm, 2011, 13, 6747.	1.3	26
209	Long-term, high-rate lithium storage capabilities of TiO2 nanostructured electrodes using 3D self-supported indium tin oxide conducting nanowire arrays. Energy and Environmental Science, 2011, 4, 1796.	15.6	76
210	Synthesis of cuprous oxide nanocomposite electrodes by room-temperature chemical partial reduction. Dalton Transactions, 2011, 40, 9498.	1.6	15
211	Highly Reversible Lithium Storage in Bacillus subtilis-Directed Porous Co <sub>3</sub> O <sub>4</sub> Nanostructures. ACS Nano, 2011, 5, 443-449.	7.3	185
212	Enhanced Li Storage Capacity in 3 nm Diameter SnO <sub>2</sub> Nanocrystals Firmly Anchored on Multiwalled Carbon Nanotubes. Journal of Physical Chemistry C, 2011, 115, 22062-22067.	1.5	76
213	Wolframite-type ZnWO <sub>4</sub> Nanorods as New Anodes for Li-Ion Batteries. Journal of Physical Chemistry C, 2011, 115, 16228-16233.	1.5	74
214	Low-temperature synthesis of CuO-interlaced nanodiscs for lithium ion battery electrodes. Nanoscale Research Letters, 2011, 6, 397.	3.1	46
215	A numerical model for vacuum carburization of an automotive gear ring. Metals and Materials International, 2011, 17, 885-890.	1.8	18
216	Fabrication of tin monosulfide nanosheet arrays using laser ablation. Applied Physics A: Materials Science and Processing, 2011, 103, 505-510.	1.1	10

#	Article	IF	CITATIONS
217	Lithium Electroactivity of Cobalt Oxide Nanoparticles Synthesized Using Thermolysis Process. Journal of the Korean Ceramic Society, 2011, 48, 636-640.	1.1	2
218	Bacteria-Mediated Synthesis of Free-Standing Cobalt Oxide Rods. Journal of Nanoscience and Nanotechnology, 2010, 10, 1129-1134.	0.9	5
219	Synthesis and photoactivity of hetero-nanostructured SrTiO3. Journal of the Ceramic Society of Japan, 2010, 118, 876-880.	0.5	15
220	Enhanced dielectric constant of polymer-matrix composites using nano-BaTiO3 agglomerates. Journal of the Ceramic Society of Japan, 2010, 118, 62-65.	0.5	8
221	Li electroactivity of iron (II) tungstate nanorods. Nanotechnology, 2010, 21, 465602.	1.3	30
222	Tailoring high-surface-area nanocrystalline TiO2 polymorphs for high-power Li ion battery electrodes. Electrochimica Acta, 2010, 55, 7315-7321.	2.6	37
223	Synthesis of Heterogeneous Li4Ti5O12 Nanostructured Anodes with Long-Term Cycle Stability. Nanoscale Research Letters, 2010, 5, 1585-1589.	3.1	36
224	Electrochemical impedance spectroscopic characterization on nano-sized Ca3Co3FeO9 electrode with enhanced capacity retention. Journal of Applied Electrochemistry, 2010, 40, 109-114.	1.5	12
225	Effects of carbon content on the photocatalytic activity of C/BiVO4 composites under visible light irradiation. Materials Chemistry and Physics, 2010, 119, 106-111.	2.0	54
226	Low-temperature sintering of temperature-stable LaNbO4 microwave dielectric ceramics. Materials Research Bulletin, 2010, 45, 21-24.	2.7	46
227	Lowâ€Temperature Synthesis of Phaseâ€Pure 0D–1D BaTiO <sub>3</sub> Nanostructures Using H <sub>2</sub> Ti <sub>3</sub> O <sub>7</sub> Templates. European Journal of Inorganic Chemistry, 2010, 2010, 1343-1347.	1.0	13
228	Superior rate capabilities of SnS nanosheet electrodes for Li ion batteries. Electrochemistry Communications, 2010, 12, 307-310.	2.3	92
229	A graphite foil electrode covered with electrochemically exfoliated graphene nanosheets. Electrochemistry Communications, 2010, 12, 1419-1422.	2.3	51
230	Facile hydrothermal synthesis of porous TiO <sub>2</sub> nanowire electrodes with high-rate capability for Li ion batteries. Nanotechnology, 2010, 21, 255706.	1.3	68
231	Facile Hydrothermal Synthesis of SrNb <sub>2</sub> O <sub>6</sub> Nanotubes with Rhombic Cross Sections. Crystal Growth and Design, 2010, 10, 2447-2450.	1.4	9
232	SrNb2O6 nanotubes with enhanced photocatalytic activity. Journal of Materials Chemistry, 2010, 20, 3979.	6.7	28
233	Enhancement of Field-Emission Properties in ZnO Nanowire Array by Post-Annealing in H <sub>2</sub> Ambient. Journal of Nanoscience and Nanotechnology, 2009, 9, 4328-4332.	0.9	16
234	On-chip fabrication of ZnO-nanowire gas sensor with high gas sensitivity. Sensors and Actuators B: Chemical, 2009, 138, 168-173.	4.0	303

#	Article	IF	CITATIONS
235	Enhanced cycling performance of an Fe0/Fe3O4nanocomposite electrode for lithium-ion batteries. Nanotechnology, 2009, 20, 295205.	1.3	58
236	Self-supported SnO <sub>2</sub> nanowire electrodes for high-power lithium-ion batteries. Nanotechnology, 2009, 20, 455701.	1.3	129
237	High rate capabilities induced by multi-phasic nanodomains in iron-substituted calcium cobaltite electrodes. Journal of Materials Chemistry, 2009, 19, 1829.	6.7	20
238	Electrochemical Performance of Calcium Cobaltite Nano-Plates. Journal of Nanoscience and Nanotechnology, 2009, 9, 4056-4060.	0.9	2
239	Morphological Evolution of CdS Nanowires to Nanosheets. Journal of Nanoscience and Nanotechnology, 2009, 9, 4487-4491.	0.9	6
240	Synthesis and Optical Properties in ZnSxSe1-x Alloy Nanowires. Journal of the Korean Physical Society, 2009, 54, 1650-1654.	0.3	7
241	Origin of Capacity Fading in Nano-Sized Co3O4Electrodes: Electrochemical Impedance Spectroscopy Study. Nanoscale Research Letters, 2008, 3, .	3.1	58
242	Preparation of Brookite‶ype TiO <sub>2</sub> /Carbon Nanocomposite Electrodes for Application to Li Ion Batteries. European Journal of Inorganic Chemistry, 2008, 2008, 878-882.	1.0	72
243	Synthesis of Cu <sub>2</sub> PO <sub>4</sub> OH Hierarchical Superstructures with Photocatalytic Activity in Visible Light. Advanced Functional Materials, 2008, 18, 2154-2162.	7.8	141
244	Visible-Light-Induced Photocatalytic Activity in FeNbO <sub>4</sub> Nanoparticles. Journal of Physical Chemistry C, 2008, 112, 18393-18398.	1.5	45
245	Gas sensing properties of defect-controlled ZnO-nanowire gas sensor. Applied Physics Letters, 2008, 93, .	1.5	643
246	Novel one-pot route to monodisperse thermosensitive hollow microcapsules in a microfluidic system. Lab on A Chip, 2008, 8, 1544.	3.1	80
247	Enhanced Rate Capabilities of Nanobrookite with Electronically Conducting MWCNT Networks. Crystal Growth and Design, 2008, 8, 4506-4510.	1.4	32
248	Stable field emission performance of SiC-nanowire-based cathodes. Nanotechnology, 2008, 19, 225706.	1.3	50
249	Sintering Behavior and Microwave Dielectric Properties of Tricalcium Phosphate Polymorphs. Japanese Journal of Applied Physics, 2007, 46, 2999-3003.	0.8	19
250	Highly Conductive Coaxial SnO <sub>2</sub> â^'ln <sub>2</sub> O <sub>3</sub> Heterostructured Nanowires for Li Ion Battery Electrodes. Nano Letters, 2007, 7, 3041-3045.	4.5	312
251	Formation of Lithiumâ€Driven Active/Inactive Nanocomposite Electrodes Based on Ca <sub>3</sub> Co <sub>4</sub> O <sub>9</sub> Nanoplates. Angewandte Chemie - International Edition, 2007, 46, 6654-6657.	7.2	75
252	Microwave dielectric properties and low-temperature sintering of Ba3Ti4Nb4O21 ceramics with B2O3 and CuO additions. Journal of the European Ceramic Society, 2007, 27, 3053-3057.	2.8	31

#	Article	IF	CITATIONS
253	Microwave dielectric properties and Far-infrared spectroscopic analysis of Ba5+nTinNb4O15+3n (0.3 <n<1.2) 2007,="" 27,="" 3081-3086.<="" ceramic="" ceramics.="" european="" journal="" of="" society,="" td="" the=""><td>2.8</td><td>14</td></n<1.2)>	2.8	14
254	Mixture behavior and microwave dielectric properties of (1â^'x)CaWO4–xTiO2. Journal of the European Ceramic Society, 2007, 27, 3087-3091.	2.8	84
255	Low temperature sintering and microwave dielectric properties of Ba3Ti5Nb6O28 with ZnO–B2O3 glass additions for LTCC applications. Journal of the European Ceramic Society, 2007, 27, 3075-3079.	2.8	26
256	Degradation Mechanism of Dielectric Loss in Barium Niobate Under a Reducing Atmosphere. Journal of the American Ceramic Society, 2006, 89, 3302-3304.	1.9	6
257	Microwave Dielectric Properties of Rare-Earth Ortho-Niobates with Ferroelasticity. Journal of the American Ceramic Society, 2006, 89, 3861-3864.	1.9	118
258	Mixture behavior and microwave dielectric properties of (1â~'x)Ca2P2O7–xTiO2. Journal of the European Ceramic Society, 2006, 26, 2007-2010.	2.8	25
259	Low-temperature sintering and microwave dielectric properties of Ba5Nb4O15 with ZnB2O4 glass. Journal of the European Ceramic Society, 2006, 26, 2105-2109.	2.8	40
260	Influence of strain on the dielectric properties of Bi–Zn–Ti–Nb–O solid solution thin films. Journal of the European Ceramic Society, 2006, 26, 2161-2164.	2.8	3
261	Virus-Enabled Synthesis and Assembly of Nanowires for Lithium Ion Battery Electrodes. Science, 2006, 312, 885-888.	6.0	1,756
262	Low temperature sintering and microwave dielectric properties of Ba3Ti5Nb6O28 with B2O3 and CuO additions. Journal of Electroceramics, 2006, 17, 439-443.	0.8	12
263	Phase transformation and microwave dielectric properties of BiPO4 ceramics. Journal of Electroceramics, 2006, 16, 379-383.	0.8	51
264	Investigation of the relations between structure and microwave dielectric properties of divalent metal tungstate compounds. Journal of the European Ceramic Society, 2006, 26, 2051-2054.	2.8	314
265	Direct Assembly of BaTiO3-Poly(methyl methacrylate) Nanocomposite Films. Macromolecular Rapid Communications, 2006, 27, 1821-1825.	2.0	24
266	A textured barium niobate with enhanced temperature stability of dielectric constant for high-frequency applications. Journal of Materials Research, 2006, 21, 2354-2360.	1.2	0
267	Crystal growth in the low-temperature deposition of polycrystalline silicon thin film. Journal of Crystal Growth, 2005, 274, 347-354.	0.7	0
268	Glass-free LTCC microwave dielectric ceramics. Materials Research Bulletin, 2005, 40, 2120-2129.	2.7	97
269	Microwave dielectric properties of (Ca1â^'xZnx)2P2O7. Materials Letters, 2005, 59, 257-260.	1.3	40
270	Voltage-Tunable Dielectric Properties of Pyrochlore Bi–Zn–Nb–Ti–O Solid-Solution Thin Films. Japanese Journal of Applied Physics, 2005, 44, 6648-6653.	0.8	20

#	Article	IF	CITATIONS
271	Influence of Anatase–Rutile Phase Transformation on Dielectric Properties of Sol–Gel Derived TiO2Thin Films. Japanese Journal of Applied Physics, 2005, 44, 6148-6151.	0.8	37
272	Low-Temperature Sintering of V2O5-Added and -Substituted ZnNb2O6Microwave Ceramics. Japanese Journal of Applied Physics, 2004, 43, 3511-3515.	0.8	20
273	Microwave Dielectric Properties of Lowâ€Fired ZnNb <sub>2</sub> O <sub>6</sub> Ceramics with BiVO <sub>4</sub> Addition. Journal of the American Ceramic Society, 2004, 87, 871-874.	1.9	98
274	Study of magnetic and magnetoelectric measurements in bismuth iron titanate ceramic—Bi8Fe4Ti3O24. Materials Research Bulletin, 2004, 39, 55-61.	2.7	72
275	Influence of V2O5 substitutions to Bi2(Zn1/3Nb2/3)2O7 pyrochlore on sintering temperature and dielectric properties. Ceramics International, 2004, 30, 1187-1190.	2.3	19
276	Low-temperature sintering and microwave dielectric properties of BaO·(Nd1â^'xBix)2O3·4TiO2 by the glass additions. Ceramics International, 2004, 30, 1181-1185.	2.3	61
277	Microwave Dielectric Properties of A2P2O7(A = Ca, Sr, Ba; Mg, Zn, Mn). Japanese Journal of Applied Physics, 2004, 43, 3521-3525.	0.8	79
278	Phase transformation and sintering behavior of Ca2P2O7. Materials Letters, 2004, 58, 347-351.	1.3	31
279	Microwave dielectric properties of Ca2P2O7. Journal of the European Ceramic Society, 2003, 23, 2589-2592.	2.8	75
280	Phase analysis and microwave dielectric properties of LTCC TiO2 with glass system. Journal of the European Ceramic Society, 2003, 23, 2549-2552.	2.8	35
281	Low-temperature sintering and microwave dielectric properties of Ba5Nb4O15–BaNb2O6 mixtures for LTCC applications. Journal of the European Ceramic Society, 2003, 23, 2597-2601.	2.8	78
282	Atmospheric Dependence on Dielectric Loss of 1/6Ba <sub>5</sub> Nb <sub>4</sub> O <sub>15</sub> · 5/6BaNb <sub>2</sub> O <sub>6</sub> Ceramics. Journal of the American Ceramic Society, 2003, 86, 795-799.	1.9	4
283	Observation of ferroelectromagnetic nature in rare-earth-substituted bismuth iron titanate. Applied Physics Letters, 2003, 83, 2217-2219.	1.5	74
284	Microwave Dielectric Properties of Bi2(Zn1/3Ta2/3)2O7Polymorphs. Japanese Journal of Applied Physics, 2003, 42, 5172-5175.	0.8	14
285	Significant changes in the ferroelectric properties of BiFeO3 modified SrBi2Ta2O9. Applied Physics Letters, 2003, 83, 1602-1604.	1.5	10
286	Influence of Substrates on the Crystal Structure of Pulsed Laser Deposited Pb(Mg1/3Nb2/3)O3–29% PbTiO3 Thin Films. Journal of Materials Research, 2002, 17, 1030-1034.	1.2	3
287	The Reversible Phase Transition and Dielectric Properties of BaNb2O6Polymorphs. Japanese Journal of Applied Physics, 2002, 41, 6045-6048.	0.8	25
288	Microwave Dielectric Properties of (1-x)Ba5Nb4O15–xBaNb2O6Mixtures. Japanese Journal of Applied Physics, 2002, 41, 3812-3816.	0.8	26

#	Article	IF	CITATIONS
289	Structural Transition and Microwave Dielectric Properties of ZnNb2O6–TiO2Sintered at Low Temperatures. Japanese Journal of Applied Physics, 2002, 41, 1465-1469.	0.8	33
290	Voltage tunable dielectric properties of rf sputtered Bi2O3-ZnO-Nb2O5 pyrochlore thin films. Thin Solid Films, 2002, 419, 183-188.	0.8	65
291	Origin of Microwave Dielectric Loss in ZnNb <sub>2</sub> 0 <sub>6</sub> â€TiO <sub>2</sub> . Journal of the American Ceramic Society, 2002, 85, 1169-1172.	1.9	55
292	Microwave Dielectric Properties of Lowâ€Fired Ba <sub>5</sub> Nb <sub>4</sub> O <sub>15</sub> . Journal of the American Ceramic Society, 2002, 85, 2759-2762.	1.9	57
293	Phase Constitutions and Microwave Dielectric Properties of Zn3Nb2O8–TiO2. Japanese Journal of Applied Physics, 2001, 40, 5994-5998.	0.8	73
294	Low-temperature firing and microwave dielectric properties of BaTi4O9 with Zn-B-O glass system. Materials Research Bulletin, 2001, 36, 585-595.	2.7	97
295	Microwave dielectric properties of (1 â^' x)Cu3Nb2O8â^'xZn3Nb2O8 ceramics. Journal of Materials Research, 2001, 16, 1465-1470.	1.2	46
296	Influence of Copper(II) Oxide Additions to Zinc Niobate Microwave Ceramics on Sintering Temperature and Dielectric Properties. Journal of the American Ceramic Society, 2001, 84, 1286-1290.	1.9	105
297	Mixture Behavior and Microwave Dielectric Properties in the Low-fired TiO2–CuO System. Japanese Journal of Applied Physics, 2000, 39, 2696-2700.	0.8	73
298	Phase Relations and Microwave Dielectric Properties of ZnNb <sub>2</sub> O <sub>6</sub> –TiO <sub>2</sub> . Journal of Materials Research, 2000, 15, 1331-1335.	1.2	117
299	Dielectric properties of Ln(Mg <sub>1/2</sub> Ti <sub>1/2</sub> )O <sub>3</sub> as substrates for high-T <sub><i>c</i></sub> superconductor thin films. Journal of Materials Research, 1999, 14, 2484-2487.	1.2	120
300	Low-firing of CuO-doped anatase. Materials Research Bulletin, 1999, 34, 771-781.	2.7	60
301	Origin of a Shrinkage Anomaly in Anatase. Journal of the American Ceramic Society, 1998, 81, 1692-1694.	1.9	18
302	Interaction of BiNbO <sub>4</sub> â€Based Lowâ€Firing Ceramics with Silver Electrodes. Journal of the American Ceramic Society, 1998, 81, 3038-3040.	1.9	54